

Theoretical Study on Water-Exchange Reactions of the Divalent and Trivalent Metal Ions of the First Transition Period

Ralf Åkesson,[†] Lars G. M. Pettersson,^{*‡} Magnus Sandström,^{*†} and Ulf Wahlgren[†]

Contribution from the Department of Chemistry, Royal Institute of Technology, S-100 44 Stockholm, Sweden, and Department of Physics, Stockholm University, P.O. Box 6730, S-113 85 Stockholm, Sweden

Received October 12, 1993. Revised Manuscript Received February 4, 1994[⊙]

Abstract: Water-exchange reactions of the hexahydrated 3d ions have been studied using large basis set SCF computations on isolated penta- (in trigonal bipyramidal or square pyramidal conformation), hexa-, and heptahydrated metal ion complexes, the latter with one single M–O distance and two angular coordinates optimized. A dissociative mechanism has been modeled by using the dissociation energy of the sixth water ligand in a gas-phase process as the activation energy in an Arrhenius plot versus the logarithm of the experimental water-exchange rate in solution, under the assumption that the energy contributions from solvent effects are similar within a series of ions. For the divalent 3d ions (V²⁺ to Zn²⁺), the remarkably good linear correlation found, in combination with the fairly constant solvation energies estimated in the preceding article, strongly supports an essentially dissociative mechanism in solution. This is not compatible with the associative interchange mechanisms proposed for Mn²⁺ and V²⁺ on the basis of their negative experimental activation volumes, ΔV^\ddagger , for which an alternative explanation is proposed. For the trivalent ions Ti³⁺, V³⁺, Cr³⁺, Fe³⁺, and Ga³⁺, the four first also with negative ΔV^\ddagger values, a corresponding plot gives a poor correlation. An associative mechanism has been investigated by using the binding energy of the seventh water ligand in a similar Arrhenius plot. The divalent 3d ions showed no correlation, supporting the previous conclusion of a dissociative mechanism. The trivalent 3d ions with negative ΔV^\ddagger values gave an acceptable correlation with an associative interchange model, while the Ga³⁺ ion previously reported to react dissociatively, deviated as expected. Comparisons of calculated and experimental activation enthalpies supported an intermediate water interchange mechanism with increasingly associative character in the order Cr³⁺, Fe³⁺, V³⁺, and Ti³⁺.

Introduction

Water-exchange reactions are a key to the understanding of complex formation and reactivity of metal ions in solution, particularly for the large variations of the rates for the transition elements.^{1,2} The mechanisms of the deceptively simple symmetrical exchange reactions of the hexahydrated ions, $[M(H_2O)_6]^{n+} + H_2O^* \rightleftharpoons [M(H_2O)_6^*]^{n+} + H_2O$, have, however, proved to be difficult to penetrate, partly because the dependence of the rate on the concentration of the entering water ligand cannot be adequately tested. Ligand sensitivity of the rate-limiting step of the complex formation is often used in mechanistic classification schemes to indicate whether the entering group has a significant influence or not on the transition state. For all the divalent 3d ions, such classifications suggested a dissociative (I_d) character with a classical Eigen–Wilkins ion-pair formation mechanism, and an appreciable associative character (I_a) for most trivalent ions.^{1–3} More recently, however, the measurements of activation parameters by high-pressure NMR methods, have given new insights into the mechanisms and the transition states. In particular, the activation volume, ΔV^\ddagger , has been used to propose the probable type of mechanism of the reactions.⁴ Nonanticipated conclusions were drawn, e.g. that the water-exchange reactions for the early transition metal ions Mn²⁺ and V²⁺ should be of associative (I_a) character, because of their negative ΔV^\ddagger values.³

However, all mechanistic interpretations of measured parameters are based on assumptions concerning the chosen model, and in order to use the ΔV^\ddagger value as a direct indicator of the type of exchange mechanism, several severe approximations have to be made. For example, volume changes due to electrostriction of the entering ligand during its penetration into the first hydration shell and due to different solvation of the transition state complex are neglected.^{4b,5} A recent example of the uncertainties introduced is provided by a study of the $[Ru(H_2O)_6]^{2+}$ ion, for which an intermediate interchange mechanism I was inferred from the small value of $\Delta V^\ddagger = -0.4 \pm 0.6 \text{ cm}^3 \text{ mol}^{-1}$, albeit the similarity of the interchange rate constants for different ligands indicates a dissociative interchange I_d mechanism.⁶ Even for the square planar $[Pd(H_2O)_4]^{2+}$ and $[Pt(H_2O)_4]^{2+}$ complexes, where associative exchange would be expected, the ΔV^\ddagger values are only moderately negative, -2.2 and $-4.6 \text{ cm}^3 \text{ mol}^{-1}$, respectively.³ Clearly, additional results from other methods are desirable in order to reach more reliable mechanistic interpretations of the observed kinetic properties of the reactions.

Recently, a gas-phase water dissociation process of the hexahydrated divalent 3d transition ions from Ca²⁺ to Zn²⁺ was modeled in a theoretical study.⁷ The lowest total energies of the pentahydrated transition states, $M(H_2O)_5^{2+}$, with trigonal bipyramidal (TBP) or square pyramidal (SQP) coordination, were compared with the corresponding hexahydrated complexes, giving the gas-phase dissociation energy of the sixth water ligand, ΔE_6 . In order to relate such a gas-phase process to the water-exchange reaction in solution, several conditions have to be met. Assuming the validity of transition-state theory, it is clear from the Arrhenius equation, $k = A \exp(-E_a/RT)$, that a plot of the dissociation

[†] Royal Institute of Technology.

[‡] Stockholm University.

[⊙] Abstract published in *Advance ACS Abstracts*, August 1, 1994.

(1) Wilkins, R. G. *Kinetics and Mechanism of Reactions of Transition Metal Complexes*, 2nd ed.; VCH: Weinheim, 1991; Chapter 4.

(2) Basolo, F.; Pearson, R. G. *Mechanisms of Inorganic Reactions*; Wiley: New York, 1967; Chapter 2.

(3) Swaddle, T. W. *Adv. Inorg. Bioinorg. Mech.* 1983, 2, 95.

(4) (a) Ducommun, Y.; Merbach, A. E. In *Inorganic High Pressure Chemistry, Kinetics and Mechanisms*; van Eldik, R., Ed.; Elsevier: Amsterdam, 1986; Chapter 2.2. (b) van Eldik, R. *Ibid.* Chapter 1. (c) van Eldik, R.; Asano, T.; le Noble, W. *J. Chem. Rev.* 1989, 89, 549.

(5) Lay, P. A. *Comments Inorg. Chem.* 1991, 9, 235.

(6) Aebischer, N.; Laurenczy, G.; Ludi, A.; Merbach, A. E. *Inorg. Chem.* 1993, 32, 2810.

(7) Åkesson, R.; Pettersson, L. G. M.; Sandström, M.; Siegbahn, P.; Wahlgren, U. *J. Phys. Chem.* 1992, 96, 10773. (b) *Ibid.* 1993, 97, 3765.

energy, ΔE_6 , vs the logarithm of the experimental rate constant, $\log k$, for exchange reactions with similar preexponential factors, A , gives a linear correlation if the dissociation energy is either (1) close to the Arrhenius activation energy, E_a , or (2) different from E_a by a constant amount in a series of ions. This idea conforms essentially to the collisional activation model in liquid solutions, which is considered virtually to be the same as in the gas phase with translational to vibrational energy transfer between the colliding molecules to achieve the transition state. Also, the assumption that the transition state corresponds to an activated complex with energy equivalence between identical aqua ligands arranged in the lowest energy conformation is in line with the view that the average molecule is in contact with another for a prolonged period while undergoing a series of collisions in a vibrational sort of way.⁸ A remarkably good correlation was obtained in such an Arrhenius plot for all divalent hexahydrated 3d ions from V^{2+} to Zn^{2+} .^{7b} This validates the above assumptions and strongly supports an essentially dissociative water-exchange mechanism for all ions in this series. The conclusion is not compatible with the proposed gradual change in mechanism in the series from associative to dissociative interchange, based on the magnitude and the change in sign from negative to positive of the corresponding activation volumes.⁴ As discussed previously,^{7b} the theoretical results are consistent with a rate-determining bond-breaking step, resulting in a pentahydrated transition state. The more negative ΔV^\ddagger values for the early transition metal ions, which have a larger size and a low occupation of the 3d $t_g(T_h)$ orbitals, are proposed to mainly reflect a deeper penetration of an incoming water molecule along the trifold axis of a face of the MO_6 coordination octahedron before a bond breaks and the five remaining water ligands rearrange to the lowest energy conformation (cf. Figure 5, ref 7b, and the discussion of the proposed mechanism). This would lead to different profiles of the energy change than of the volume change during the water-exchange reaction, i.e. the compaction necessary to achieve the transition state does not necessarily correspond to the energetics of the bond making/breaking.

Previously, the binding energies have been obtained in the highest possible symmetry for the hexahydrated ions, i.e. T_h or D_{2h} for Jahn–Teller distorted ions.^{7a,9,10} Other conformations of the water ligands (in D_{3d} symmetry), which particularly for large d^1 and d^2 ions can give higher binding energy, have also been considered both for the divalent and trivalent 3d elements.⁹ In the present study, the energy of a heptahydrated metal ion representing the transition state has been calculated, in order to model an associative exchange mechanism. The calculated (gas-phase) dissociation energy of the seventh water ligand, ΔE_7 for $M(H_2O)_7^{n+} \rightarrow M(H_2O)_6^{n+} + H_2O$, has been compared with experimental data in a way similar to that for the dissociative model. In addition to the heptahydrates of all divalent 3d ions from Ca^{2+} to Zn^{2+} , the trivalent 3d ions Ti^{3+} , V^{3+} , Cr^{3+} , Fe^{3+} , and Ga^{3+} , for which both the experimental rate constants and activation volumes of solvent exchange reactions in water are known, have been studied. Also Sc^{3+} , which has been studied in nonaqueous solvents,⁴ and Mn^{3+} are included for comparisons. The rate constants cover an extremely wide range, from 2.4×10^{-6} (Cr^{3+}) to 1.8×10^5 (Ti^{3+}), although the ΔV^\ddagger values are negative for all these ions except Ga^{3+} (see Table 3). The higher charge for the trivalent ions leads to shorter M–O distances and higher binding energies than for the divalent ions of the same elements and also larger ligand-field stabilization energies, as discussed in the preceding article.⁹ Before precise measurements of the activation volumes became available, the prevalent view of the water-exchange reactions was that the dominating

mechanisms were dissociative for the divalent hexahydrated ions and mainly associative for most trivalent ions due to their stronger attraction of an outer-sphere water molecule.^{1,3} The energy correlations in this study largely support this view, and the proposed exchange models can also qualitatively account for the variations found in the activation volumes.

Methods

Models. For the pentahydrated complexes $[M(H_2O)_5]^{3+}$, $M = Sc^{3+}$, Ti^{3+} , V^{3+} , Cr^{3+} , Mn^{3+} , Fe^{3+} , and Ga^{3+} , we have optimized the bond distances to obtain the energy minima with the use of ab initio SCF methods in a way similar to that for the divalent ions.^{7b} Two limiting stereochemical conformations have been considered: (1) square pyramidal (SQP) with optimizations of the R_{ax} , R_{eq} , and R_{pyr} distances and (2) trigonal bipyramidal (TBP) for which the axial (R_{ax}) and equatorial (R_{eq}) metal–oxygen distances were optimized (see Figure 1a,b).

The relation between the structure of the heptahydrated metal ions, $[M(H_2O)_7]^{n+}$, and the T_h symmetry of the hexahydrates (cf. Figure 1 and ref 9) can be seen in Figure 1c. The axial apex water molecule in an MO_6 octahedron has been replaced by two ligands with their separation defined by the angle α , and the resulting bend-away movement due to the repulsion of the equatorial ligands is defined by β . In line with the view that in solution the transition state along the symmetrical reaction path persists for a rather long time on the collisional time scale,^{8,11} energy equivalence between the seven ligands should be obtained. A relatively high symmetry (C_{2v}) can be kept, giving a reasonable size of the computations, with the geometry optimizations restricted to three parameters: a single mean M–O distance (R_7) and two angular coordinates α and β (Figure 1c).

A trigonal planar coordination of the water molecules has been assumed throughout, with the internal water geometry as previously kept at the gas-phase values ($R(O-H) = 0.957 \text{ \AA}$, $HOH = 104.5^\circ$).^{7,9,10}

A slightly different structure, henceforth denoted the "alternative" structure, used by Hermansson and Probst for calculations on heptahydrated metal ions (with two additional hydrogen-bonded second sphere water molecules),¹² has also been considered. It differs from our chosen structure in two respects: the axial water molecules are rotated 45° about the z -axis (Figure 1) to be located diagonally between the equatorial water molecules, which are all oriented vertically in order to maintain the C_{2v} symmetry of the complex. However, optimizations of the $[Mn(H_2O)_7]^{2+}$ complex in both conformations resulted in only slightly longer R_7 values (optimized geometry: $R_7 = 2.344 \text{ \AA}$, $\alpha = 73.3^\circ$, $\beta = 77.4^\circ$), but significantly higher total energy, $\sim 27 \text{ kJ mol}^{-1}$, for this "alternative" structure. One unfavorable feature seems to be the Pauli repulsion between the oxygen lone pairs, resulting in an antibonding $O_{ax}-O_{eq}$ overlap (mainly $O_{ax} p_z$ and $O_{eq} p_x, p_y$), which is more pronounced for the "alternative" than for the chosen structure, -0.22 and $-0.12 e^-$, respectively. Also, the orientation of the water molecules is less favorable and previous experience shows the repulsion between the hydrogen atoms to be important (cf. "eclipsed TBP" in ref 7b with $\sim 10\text{--}30 \text{ kJ mol}^{-1}$ smaller binding energy values than for the most favorable TBP conformation). In order to test the influence of a higher charge on the structure, single-point calculations were performed on $[Fe(H_2O)_7]^{3+}$ and $[Ga(H_2O)_7]^{3+}$ in the "alternative" geometry (with estimated R_7 , α , and β), giving energies of a similar magnitude ($20\text{--}25 \text{ kJ mol}^{-1}$) above those of the chosen structure.

The $[M(H_2O)_7]^{n+}$ structure can be related to a pentagonal bipyramid, and with the α and β angles equal to 72° , a regular MO_5 base plane is formed with two distorted "axial" ligands, cf. Figure 1c. However, a regular pentagonal bipyramidal structure with vertical water ligands in the base plane ($M-O_{eq} 2.285$, $M-O_{ax} 2.181 \text{ \AA}$) gave 42 kJ mol^{-1} higher energy for Sc^{3+} .

Basis Sets and Computation Methods. The same basis sets as in the previous studies of the penta- and hexahydrated ions were used.^{8–10} The shorter M–O distances for the trivalent ions combined with the high charge state give rise to larger basis set superposition errors (BSSE) and require slightly larger basis sets than those used for the corresponding dipositive ions.⁹ Two additional functions (s and p) were left uncontracted which resulted in a contracted (6s5p3d) metal basis and gave a BSSE of $<100 \text{ cm}^{-1}$ for the hexahydrates.⁹ In the present study, the BSSE for $[Ga(H_2O)_5]^{3+}$, which has the shortest M–O distance and therefore should be the most unfavorable case, was investigated and gave an acceptably low value, 2.1 kJ mol^{-1} (173 cm^{-1}).

(8) Bockris, J. O'M.; Khan, S. U. M. *Quantum Electrochemistry*; Plenum: New York, 1979; Chapter 2.1–2.3.

(9) Åkesson, R.; Pettersson, L. G. M.; Sandström, M.; Wahlgren, U. *J. Am. Chem. Soc.*, preceding article in this issue.

(10) Åkesson, R.; Pettersson, L. G. M.; Sandström, M.; Wahlgren, U. *J. Phys. Chem.* **1992**, *96*, 150.

(11) Swaddle, T. W. *Comments Inorg. Chem.* **1991**, *12*, 237.

(12) Probst, M.; Hermansson, K. *J. Chem. Phys.* **1992**, *12*, 8995.

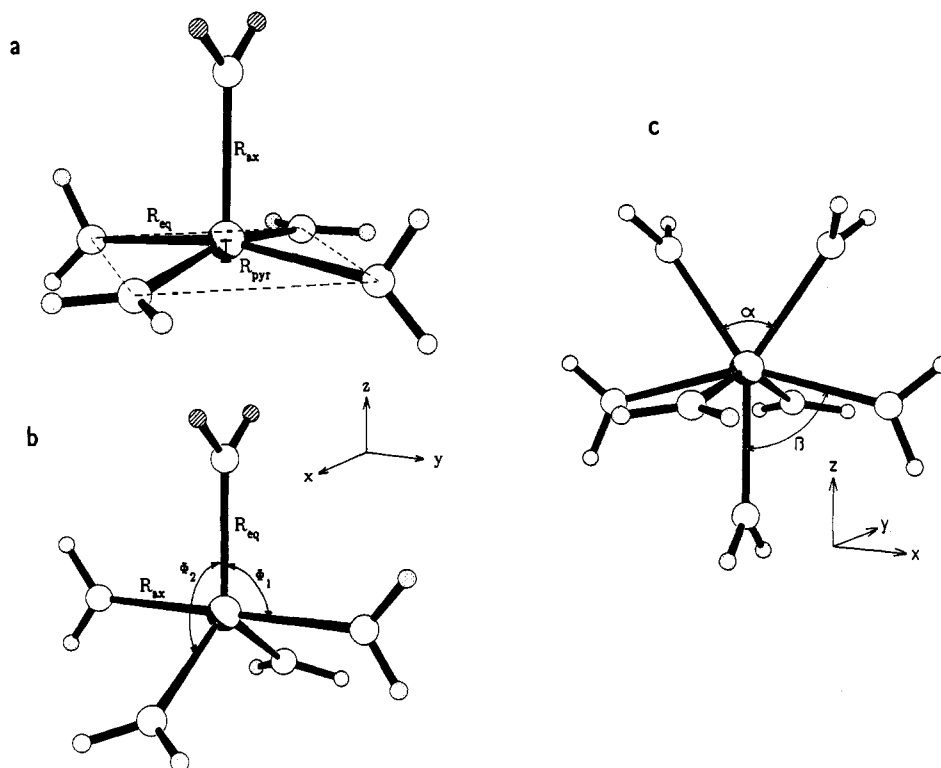


Figure 1. Models of the hydrated ions defining the refined parameters and the coordinate system: the pentahydrated ions in (a) trigonal bipyramidal TBP and (b) square pyramidal SQP geometries and (c) the heptahydrated ion.

The geometry optimizations were performed using the MOLECULE-SWEDEN system of programs¹³ with the medium-sized O/H basis set. The energy of the optimized structure was then recomputed using a modified version of the direct SCF program DISCO^{14,15} running on a Cray X-MP/416, with a larger water basis set (including two d functions on oxygen and one p function on hydrogen), as in the previous studies. The larger basis set gives a dipole moment and dipole polarizability of H₂O close to the Hartree–Fock limit,¹⁰ which is important for reliable estimates of the energy barriers. The previous studies showed that structures optimized with the larger water basis set give slightly longer (<0.02 Å) bond lengths than with the medium-sized basis set but very small relative energy changes along the period.^{7,9} For the trivalent [M(H₂O)₇]³⁺ systems, the calculations with the large water basis set required a total of 298 basis functions.

For the divalent [M(H₂O)₇]²⁺ clusters, the basis sets and contraction method were the same as those used before.^{7b} In this case, however, an extrapolation of the differences of the binding energies for M(H₂O)_n^{m+} ($n = 5-7$, $m = 2, 3$) with the large and medium-sized basis sets, together with a calibration calculation in one case, [Mn(H₂O)₇]²⁺, was considered sufficient to relate them to the level expected for the large water basis set. A correction reducing all the ΔE_7 values of the divalent ions by ~ 8.2 kJ mol⁻¹ was estimated in this way.

The trends and variations in the binding energies of the series of transition metal ion hydrates with their electrostatically dominated bonding have been shown to be adequately reproduced by calculations at the SCF level.⁹ This has also been verified by model calculations on the corresponding series of mono- and dihydrated divalent ions, where electron correlation of the water valence and metal 3d orbitals merely shifted the binding energy curve by a nearly constant amount.¹⁶ For the hydrated V³⁺ and Co²⁺ ions, CASSCF calculations with the medium O/H basis sets were performed with the 3d orbitals in the active space,

since a two-determinant wave function is necessary to account for the contribution from the atomic ground state of the ions.^{7,9} The correction $\Delta E_{\text{CAS}} = E_{\text{SCF}} - E_{\text{CAS}}$, which was subtracted from the single-configuration large-basis SCF energies, was for [V(H₂O)₅]³⁺ (19.00 (TBP) and 14.58 (SQP)), [V(H₂O)₆]³⁺ (17.69), [V(H₂O)₇]³⁺ (16.67), [Co(H₂O)₆]²⁺ (30.0), and [Co(H₂O)₇]²⁺ (29.59 kJ mol⁻¹).

Results and Discussion

Bond Lengths. Figure 2a shows the variation of the M–O distances for the lowest energy conformations of the penta-, hexa-, and heptahydrates along the series of divalent 3d ions. In all cases, maxima are found for the Ca²⁺, Mn²⁺, and Zn²⁺ ions which have no additional ligand field stabilization due to the splitting of the energy levels of the 3d orbitals. For the high-spin hexahydrates, pronounced minima were found at V²⁺ and Ni²⁺, and at Cr³⁺ and Cu³⁺, because for these ions an additional d electron enters an antibonding e_g(T_h) orbital.⁹ For the pentahydrates, the minima at Cr²⁺ and Cu²⁺ are noteworthy and correspond to their relatively high stability in the SQP ligand field (see the discussion of energy differences, ΔE_6 , below). The smoother curve for the heptahydrates, with an almost constant R_7 (M–O) distance from Fe²⁺ to Zn²⁺, reflects the more uniform interactions between the d orbitals and the more irregularly distributed ligands.

For the penta- and heptahydrates of the trivalent ions, only the first parts of the series (Sc³⁺ to Fe³⁺ and Ga³⁺) have been investigated in the present work and the optimized parameters are given in Tables 1 and 2. Similar ligand-field-induced variations are found in the bond lengths of the penta- and hexahydrates for trivalent ions of the same d electron occupancy as the divalent, although with the corresponding M–O distances reduced by 0.14–0.21 Å. Distinct minima occur at Cr³⁺ and Cu³⁺ for the hexahydrates, while Mn³⁺ gives the shortest M–O distance for the early trivalent pentahydrated transition elements (Figure 2b). The corresponding heptahydrated trivalent ions do not show an equally smooth variation of the M–O distances as in the divalent, and slightly larger R_7 values were obtained for the Ti³⁺ and Mn³⁺ ions than expected from the trend.

(13) MOLECULE-SWEDEN is an electronic structure program written by J. Almlöf, C. W. Bauschlicher, M. R. A. Blomberg, D. P. Chong, A. Heiberg, S. R. Langhoff, P.-A. Malmqvist, A. P. Rendell, B. O. Roos, P. E. M. Siegbahn, and P. R. Taylor.

(14) Almlöf, J.; Faegri, K., Jr.; Forsell, K. *J. Comput. Chem.* **1982**, *3*, 385.

(15) Saebø, S.; Almlöf, J. *Chem. Phys. Lett.* **1987**, *154*, 521.

(16) Åkesson, R.; Pettersson, L. G. M. *Chem. Phys.* **1994**, *184*, 85.

(17) Eigen, M. *Pure Appl. Chem.* **1963**, *6*, 105.

(18) van Eldik, R.; Gaede, W.; Cohen, H.; Meyerstein, D. *Inorg. Chem.* **1992**, *31*, 3695.

(19) Powell, D. H.; Helm, L.; Merbach, A. E. *J. Chem. Phys.* **1991**, *95*, 9258.

Table 1. Energy-Optimized Geometries of Trivalent Pentahydrates $M(H_2O)_5^{3+}$

ion	R_5^a	$R_{ax}(M-O)$	$R_{eq}(M-O)$	R_{pyr}	$q(M)^b$
(a) Trigonal Bipyramidal Structure ^c					
Sc ³⁺	2.136	2.153	2.125		+2.36
Ti ³⁺	2.074	2.087	2.066		+2.29
V ³⁺	2.029	2.073	1.999		+2.20
Cr ³⁺	2.008	2.004	2.010		+2.11
Fe ³⁺	2.015	2.038	2.000		+1.98
Ga ³⁺	1.943	1.975	1.921		+1.82
(b) Square Pyramidal Structure ^d					
Ti ³⁺	2.077	2.10	2.071	0.23	+2.27
V ³⁺	2.035	2.06	2.030	0.19	+2.18
Cr ³⁺	1.998	1.96	1.999	0.20	+2.06
Mn ³⁺	1.988	2.088	1.963	0.24	+2.01
Fe ³⁺	2.016	1.99	2.023	0.41	+1.98
Ga ³⁺	1.914	1.88	1.923	0.37	+1.83

^a Mean value of M–O distances in Å. ^b Metal atom charge according to Mulliken population analysis (medium size O/H basis sets). ^c See Figure 1b. ^d R_{pyr} is the height of the metal atom above the pyramidal base plane (see Figure 1a).

Table 2. Energy-Optimized Geometries^a of Divalent and Trivalent Heptahydrated $M(H_2O)_7^{n+}$ Complexes

ion	R_7	α	β	$q(M)$
(c) Heptahydrates				
Sc ³⁺	2.254	71.1	76.2	+2.52
Ti ³⁺	2.207	70.2	75.8	+2.47
V ³⁺	2.153	70.2	76.5	+2.36
Cr ³⁺	2.145	68.6	77.7	+2.22
Mn ³⁺	2.153	70.3	76.6	+2.10
Fe ³⁺	2.152	71.1	76.3	+2.01
Ga ³⁺	2.106	68.6	76.5	+2.14
Ca ²⁺	2.472	71.5	76.0	+2.02
Sc ²⁺	2.383	68.5	77.2	+1.96
Ti ²⁺	2.356	70.9	76.4	+1.92
V ²⁺	2.338	69.0	77.8	+1.85
Cr ²⁺	2.336	70.5	76.6	+1.79
Mn ²⁺	2.340	70.0	76.0	+1.74
Fe ²⁺	2.277	70.6	74.8	+1.68
Co ²⁺	2.262	70.9	76.0	+1.61
Ni ²⁺	2.250	70.0	76.0	+1.58
Cu ²⁺	2.252	71.5	76.1	+1.56
Zn ²⁺	2.255	69.9	76.2	+1.54

^a R_7 is the M–O distance in Å, and α and β are given in degrees (see Figure 1c).

For trivalent ions in SQP pentahydrates, the R_{pyr} values are as a rule larger than those for the corresponding divalent ions, for which values in the range 0.08–0.18 Å were obtained.^{7b} It seems that the large R_{pyr} values, especially for Fe³⁺ (0.41 Å) and Ga³⁺ (0.37 Å), are related to short M–O distances, giving an increase in the O_{ax} – O_{eq} repulsion, which is enhanced by the population of the antibonding d orbitals; in the case of Ga³⁺, the increased covalency probably also contributes.⁹ In all cases, the O_{ax} –M– O_{eq} angle is close to 103.6°, which corresponds to a minimum in interligand repulsion for monoatomic ligands and $R_{ax} = R_{eq}$.

Energies of Pentahydrates. The optimized SQP and TBP structures (Table 1) are generally close in energy for the trivalent ions (Table 3) and the TBP geometry is slightly favored for Ti³⁺, V³⁺, Fe³⁺, and Ga³⁺, whereas for Cr³⁺, our calculations show the SQP geometry to be the more stable with $R_{eq} > R_{ax}$ of the complex. This is a result of the ligand-field effects in a way similar to that for the corresponding isoelectronic divalent ions,^{7b} and for the Jahn–Teller active ion Mn³⁺, only the SQP structure was considered as it should be lower in energy. For the ions with no additional ligand-field stabilization, i.e. Sc³⁺, Fe³⁺, and Ga³⁺, the lower overall ligand–ligand repulsion favors the TBP structure in which $R_{eq} < R_{ax}$ because of the smaller repulsion between the equatorial ligands, as for the isoelectronic divalent Ca²⁺, Mn²⁺, and Zn²⁺ ions. No calculation was performed on [Sc(H₂O)₅]³⁺

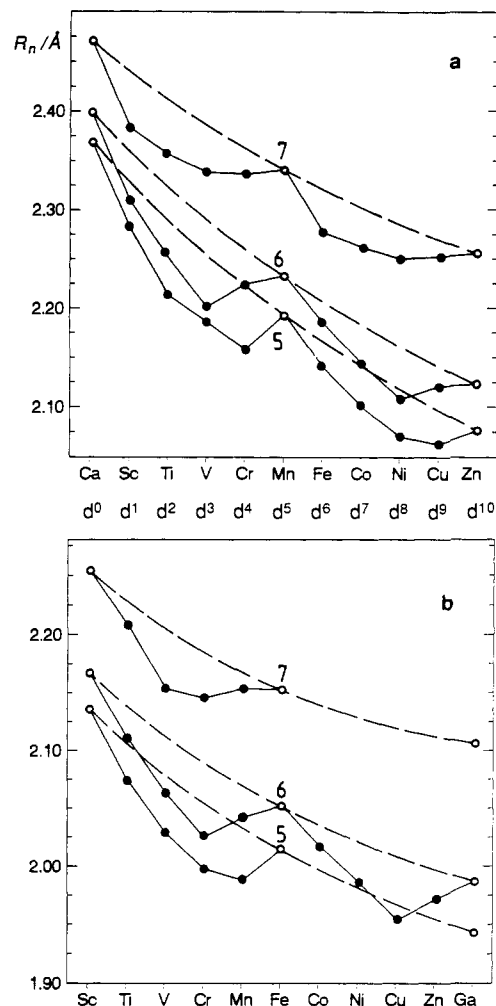


Figure 2. Ligand-field effects on the calculated M–O distances (R_n (Å)) of the (a) divalent and (b) trivalent high-spin 3d ions in penta- (lower), hexa- (middle), and heptahydrates (upper curve). The dashed lines connect the d^0 , d^5 , and d^{10} ions (open circles) with no additional ligand-field stabilization.

in the SQP geometry since by analogy with [Ca(H₂O)₅]²⁺ the TBP geometry should be clearly favored.

The slightly favored TBP conformation for the [V(H₂O)₅]³⁺ cluster is a consequence of the contribution (about 10%) of the $d_{x^2-y^2}$ orbital to the secondary determinant of the CAS calculation (see Methods). This orbital is strongly antibonding for SQP but slightly bonding in an idealized TBP structure.²

In all cases, for the trivalent ions, the elongated TBP conformation ($R_{eq} < R_{ax}$) was found to be more stable than the compressed (except for Cr³⁺), analogous to the previous study.

The highest stabilization due to the ligand-field splitting of the d-orbital energy levels is obtained for the pentahydrated Cr²⁺, Cu²⁺, and Mn³⁺ ions (Figure 3), which causes the energy differences, ΔE_6 , between penta- and hexahydrates to be the smallest in the series for these d^4 and d^9 ions which have Jahn–Teller distorted hexahydrates (Table 3).¹⁰ Thus, the stability of these pentahydrates, and not the Jahn–Teller distortion of the hexahydrates, is the reason for the high water-exchange rates of the Cu²⁺ and Cr²⁺ ions as compared to the neighboring ions (see Dissociative Mechanism, below).

Energies of Heptahydrates. A calculation of the orbital energies for [Mn(H₂O)₇]²⁺, for which all metal 3d orbitals are singly occupied in the ground state, was made to illustrate the ligand-field splittings for a heptahydrated metal ion. The d orbitals have rather pure atomic character as in the penta- and hexahydrates, with the energy order as follows: d_{xy} (–11.96), d_{xz} (–11.93),

Table 3. Experimental Rate Constants k^a , Activation Volumes $\Delta V^*_{\text{exp}}^{a,b}$ for Water-Exchange Reactions, Calculated Volume Changes, and Dissociative Activation Energies at the Formation of Pentahydrated $[M(\text{H}_2\text{O})_5]^{n+}$ Clusters ($n = 2, 3$)

M^{n+}	k (s ⁻¹)	ΔV^*_{exp}	R_6^c	$\Delta \bar{R}_{5-6}^c$	ΔV_{5-6}^d	ΔE_6^e	$\Delta H_{5-6}^{\text{soliv } f}$	$\Delta H^*_{\text{diss}}^g$	$\Delta E_{\text{TBP-SQP}}^h$	
(a) Trivalent 3d Ions										
Sc ³⁺			2.167	-0.031	-3.0	231.1	-15.3	171.8		TBP
Ti ³⁺	1.8×10^5	-12.1	2.110	-0.036	-3.3	231.6	-18.3	169.3	-2.2	TBP
V ³⁺	5.0×10^2	-8.9	2.063	-0.034	-3.1	238.8 ⁱ	-17.8	177.0	-7.8	TBP
Cr ³⁺	2.4×10^{-6}	-9.6	2.025	-0.027	-2.4	262.3	-14.4	203.9	30.9	SQP
Mn ³⁺			2.042	-0.054	-4.8	205.1	-28.8	132.3		SQP
Fe ³⁺	1.6×10^2	-5.4	2.052	-0.037	-3.3	232.4	-19.6	168.8	-0.5	TBP
Ga ³⁺	4.0×10^2	+5.0	1.987	-0.044	-3.8	217.9	-24.2	149.7	-3.0	TBP
(b) Divalent 3d Ions										
Ca ²⁺	$\sim 10^8$ ⁱ		2.399	-0.029	-3.1	116.7	-5.6	67.1	-2.9	TBP
Sc ²⁺			2.309	-0.025	-2.6	114.7	-5.0	65.7	2.1	SQP
Ti ²⁺			2.253	-0.038	-3.8	123.7 ⁱ	-8.0	71.7	-1.1	TBP
V ²⁺	87	-4.1	2.201	-0.015	-1.5	139.9	-3.2	92.7	17.9	SQP
Cr ²⁺	$\sim 7 \times 10^9$		2.225	-0.067	-6.5	98.6	-14.3	40.3	11.3	SQP
Mn ²⁺	2.1×10^7	-5.4	2.233	-0.040	-4.0	114.9	-8.5	62.4	-5.6	TBP
Fe ²⁺	4.4×10^6	+3.8	2.185	-0.045	-4.3	114.9	-9.8	61.1	-1.9	TBP
Co ²⁺	3.2×10^6	+6.1	2.143	-0.043	-4.0	116.5 ⁱ	-9.6	62.9	-6.5	TBP
Ni ²⁺	3.2×10^4	+7.2	2.108	-0.038	-3.5	129.5	-8.7	76.8	8.7	SQP
Cu ²⁺	4.4×10^9		2.121	-0.059	-5.4	103.0	-13.4	45.6	3.3	SQP
Zn ²⁺	$\sim 2 \times 10^7$		2.123	-0.057	-4.4	110.1	-10.6	55.5	-9.2	TBP

^a Reference 4. ^b cm³ mol⁻¹. ^c The mean M-O distances R_5 (Table 1) and R_6 (refs 7 and 9) give the calculated contraction $\Delta \bar{R}_{5-6} = R_5 - R_6$ (Å). ^d Volume contraction at the formation of the pentahydrated complex (cm³ mol⁻¹), assuming spherical species: $\Delta V^*_{5-6} = \frac{4}{3}\pi(R_5 + R(\text{H}_2\text{O}))^3 - \frac{4}{3}\pi(R_6 + R(\text{H}_2\text{O}))^3$, with $R(\text{H}_2\text{O}) = 1.40$ Å. ^e Calculated large water basis gas-phase bond dissociation energy $\Delta E_6 = E\{M(\text{H}_2\text{O})_5^{n+}\} + E\{\text{H}_2\text{O}\} - E\{M(\text{H}_2\text{O})_6^{n+}\}$ (kJ mol⁻¹). ^f Difference in hydration enthalpy calculated using the Born equation (ref 22) for $R_5 + R(\text{H}_2\text{O})$ and $R_6 + R(\text{H}_2\text{O})$, with $R(\text{H}_2\text{O}) = 1.40$ Å, $\epsilon = 78$, and $T\epsilon^{-1}(\partial\epsilon/\partial T) = -1.357$ for water at 298 K (ref 23). ^g Calculated dissociation activation enthalpy $\Delta H^*_{\text{diss}} = \Delta E_6 - \Delta H_{\text{vap}} + \Delta H_{5-6}^{\text{soliv}}$ (see eq 1). ^h Energy difference between TBP and SQP structures (kJ mol⁻¹) with the stable conformation given explicitly. ⁱ Calculated including the ΔE_{CAS} correction (see Methods and refs 7 and 9).

d_{yz} (-11.84), d_{1a_1} (-11.84), d_{2a_1} (-11.83 eV) (the two latter are denoted by their symmetry species since the relative contributions from $d_{x^2-y^2}$ and d_{z^2} may change due to orbital rotations; the coordinate system is defined in Figure 1c). A similar grouping of two orbitals with lower and three with higher energy is also found for the one-electron d-orbital energy levels of a pentagonal bipyramid (pyramid base in the xy plane): d_{xy} and d_{yz} (-5.28), d_{xy} and $d_{x^2-y^2}$ (+2.82), and d_{z^2} (+4.93) (in D_q units).² The same qualitative picture of the ground-state d-orbital structure was found for all heptahydrated metal ions. For $[\text{Cr}(\text{H}_2\text{O})_7]^{2+}$, the singly occupied orbital is $\sim d_{z^2-x^2}$, whereas for $[\text{Cu}(\text{H}_2\text{O})_7]^{2+}$, its character is $\sim d_{yz-x^2}$.

Mulliken population analyses in all cases showed the total 3d occupations to be close to the formal metal ion electron configuration (usually within 0.3 e⁻ with the largest difference for Sc³⁺, +0.36), with similar values for the penta-, hexa-, and heptahydrates.^{7,9}

In a calculation of the dissociation energy of the seventh ligand, $\Delta E_7 = E\{M(\text{H}_2\text{O})_6^{n+}\} + E\{\text{H}_2\text{O}\} - E\{M(\text{H}_2\text{O})_7^{n+}\}$, the lowest energies of the hexa- and heptahydrated ions in optimized geometries have been used. The calculated ΔE_7 energies for the trivalent and divalent ions, respectively (Table 4), are generally small, and for the bigger ions (cf. Figure 2), the heptahydrated gas-phase clusters are more stable (positive ΔE_7 values) than the hexahydrated ones (Figure 3). The ions with high ligand-field stabilization in their hexahydrates, i.e. Cr³⁺, V²⁺, and Ni²⁺, show for their size (R_6) low ΔE_7 values. This is a consequence of the more uniform ligand-field effects in the heptahydrates, as is shown by the corresponding smooth binding energy curves in Figure 3. The slope of the dashed curves connecting the ions without additional stabilization from the splitting of the d-orbital energies is also less steep for the heptahydrates, reflecting the increasing ligand-ligand repulsion for the smaller ions. However, the calculated values refer to a hypothetical gas-phase reaction at 0 K and additional terms have to be added to relate them to a solution reaction, as will be discussed later, i.e. solvent effects on the different gas-phase species, temperature-dependent corrections, etc.,^{7,9} which will in general increase the relative stability of the hexahydrated (and pentahydrated) species in solution. Noteworthy is that the Ca²⁺ and Sc³⁺ ions which are reported

to have higher hydration numbers than 6 in solution (see preceding article)⁹ also are the ions with the highest relative stability of the heptahydrated species in the gas phase.

Correlation with Experimental Water-Exchange Rates. I. Dissociative Mechanism. The dissociation energy of the sixth water ligand, $\Delta E_6 = E\{M(\text{H}_2\text{O})_5^{n+}\} + E\{\text{H}_2\text{O}\} - E\{M(\text{H}_2\text{O})_6^{n+}\}$, has been used as a measure of the activation energy in logarithmic Arrhenius plot against the water-exchange rate constant, $k = A \exp(-\Delta E_6/RT)$ (see Figure 4a,c). This is in effect a test of whether a dissociative gas-phase process would show a rate dependence similar to that of the solution exchange and, thus, if the assumptions made in the model are valid. As reported previously, a satisfactory linear correlation ($r_{\text{corr}} = 0.990$ with a slope -5.14 kJ mol⁻¹ of the line corresponding to a temperature of 268 K) was found for the divalent ions,^{7b} which also implies that the differences in energy contributions induced by the surrounding solvent between the initial and transition states (by hydrogen bonding and polarization) are of similar magnitude along the series of hydrated ions.

A dissociative reaction was considered in the same way for the trivalent ions. All hexahydrated trivalent 3d ions (except the Jahn-Teller distorted Mn³⁺) were previously found to have their lowest energy values in regular T_h symmetry.⁹ The dissociation energies ΔE_6 obtained with the large water basis set are given in Table 3. The correlation in Figure 4c for the trivalent 3d ions is obviously much worse than that of the regression line for the divalent ions V²⁺, Cr²⁺, Mn²⁺, Fe²⁺, Co²⁺, Ni²⁺, Cu²⁺, and Zn²⁺ (Figure 4a). This is as expected, since there are many indications of an associative behavior for most trivalent ions.^{3,4c} An exception is the Ga³⁺ ion which has been proposed to react according to a dissociative interchange mechanism, mainly on the basis of its positive activation volume, ΔV^* (cf. Table 3).^{4a} The bond contraction which takes place at the dissociation of a water molecule from its hexahydrate is relatively large, $\Delta R = -0.044$ Å (Table 3). This would correspond to a substantial volume correction ΔV_{5-6} of -3.8 cm³ mol⁻¹, which should be subtracted (as also the unknown solvent contraction term ΔV_{soliv} should be) from the experimental ΔV^* value (5.0 cm³ mol⁻¹) to obtain the intrinsic activation volume at the transition state. A fairly large positive intrinsic volume change would then be the result,

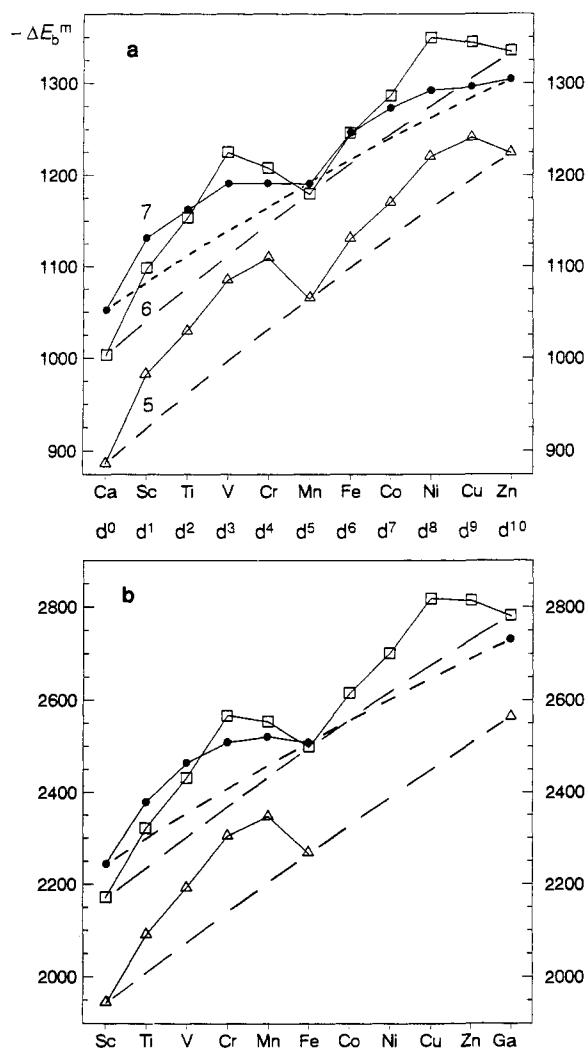


Figure 3. Binding energies $\Delta E_b^m = E\{M(H_2O)_m\} - E\{M^{n+}\} - mE\{H_2O\}$ (kJ mol^{-1}) (computed at the SCF level) for penta- ($m = 5$, triangles), hexa- ($m = 6$, squares), and heptahydrated ($m = 7$, points) high-spin 3d ions for (a) divalent ($n = 2$, upper part) and (b) trivalent ($n = 3$, lower part) ions. The ΔE_b^6 values are from Table 4, ref 9 (preceding article), and the $\Delta E_b^5 = \Delta E_b^6 - \Delta E_6$ and $\Delta E_b^7 = \Delta E_b^6 + \Delta E_7$ values are then derived from Tables 3 and 4 (this work), respectively. The dashed curves connect the d^0 , d^5 , and d^{10} ions without additional ligand-field stabilization effects from d-orbital splitting.

underlining the dissociative character of the water exchange for Ga^{3+} . A line can then be drawn through the Ga^{3+} value with a slope $RT \ln 10$ corresponding to $T = 298 \text{ K}$ (Figure 4c). Other ions with similar dissociative reactions would then follow the same correlation, under the same assumptions as for the divalent ions. The line passes close to the Cr^{3+} value, but the V^{3+} , Fe^{3+} , and Ti^{3+} ions deviate as could be expected from the mechanistic considerations.

II. Associative Mechanism. An Arrhenius plot of $k = A \exp(-\Delta E_7/RT)$, using $-\Delta E_7$ as the activation energy for an associative (gas-phase) process with a 7-coordinated transition state, gives, however, an acceptable linear fit (correlation coefficient of 0.988 for the line $\Delta E_7 = 10.42 \log k - 1.656$ (kJ mol^{-1})) for the trivalent ions if Ga^{3+} is excluded (Figure 4d). However, the slope of the correlation line for the experimental solution rate constants is too steep and would correspond to a temperature of ca. 544 K, provided that the preexponential factors A are similar for the individual water-exchange reactions. This indicates that the gas-phase binding energies ($-\Delta E_7$) and the solution activation energies do not differ with a constant amount for the four ions in the correlation. Nevertheless, the correlation in combination with other available evidence (e.g., activation volumes) is consistent

Table 4. Calculated Volume Changes and Associative Activation Energies at Formation of Heptahydrated $[M(H_2O)_7]^{n+}$ ($n = 2, 3$) Clusters

M^{n+}	$\Delta \bar{R}_{7-6}^a$	ΔV_{7-6}^b	ΔE_7^c	$\Delta H_{7-6}^{\text{soliv}}^d$	ΔH_{ass}^e	ΔH^f
(a) Trivalent 3d Ions						
Sc^{3+}	0.087	8.7	72.7	41.5	12.8	
Ti^{3+}	0.097	9.3	57.3	47.7	34.4	43.4
V^{3+}	0.090	8.4	31.7 ^g	45.5	57.8	49.4
Cr^{3+}	0.120	11.0	-58.3	61.5	163.8	108.6
Mn^{3+}	0.111	10.2	-32.0	56.5	132.5	
Fe^{3+}	0.100	9.3	9.9	50.7	84.8	64.0
Ga^{3+}	0.119	10.7	-48.4	62.4	154.8	67.1
(b) Divalent 3d Ions						
Ca^{2+}	0.073	8.1	49.1	13.7	8.6	
Sc^{2+}	0.076 ^h	7.8	33.8 ^h	14.6	24.8	
Ti^{2+}	0.104 ^h	10.8	9.1 ^{g,h}	21.0	55.9	
V^{2+}	0.137	14.0	-33.8	28.1	105.9	61.8
Cr^{2+}	0.111	11.4	-16.7	22.7	83.4	
Mn^{2+}	0.107	11.0	11.5	21.8	54.3	32.9
Fe^{2+}	0.092	9.2	1.0	19.3	62.3	41.4
Co^{2+}	0.119	11.7	-13.9 ^g	25.4	83.3	46.9
Ni^{2+}	0.142	13.8	-57.4	30.6	132.0	56.9
Cu^{2+}	0.131	12.8	-48.2	28.2	120.4	11.5
Zn^{2+}	0.132	12.9	-29.2	28.3	101.5	

^a Increase of mean M-O distances $\Delta \bar{R}_{7-6} = R_7 - R_6$ (\AA) (Tables 2 and 3). ^b Volume increase ($\text{cm}^3 \text{ mol}^{-1}$), assuming spherical species: $\Delta V_{7-6}^b = \frac{4}{3}\pi(R_7 + R(\text{H}_2\text{O}))^3 - \frac{4}{3}\pi(R_6 + R(\text{H}_2\text{O}))^3$, with $R(\text{H}_2\text{O}) = 1.40 \text{ \AA}$. ^c Binding energy of the seventh ligand $\Delta E_7 = E\{M(H_2O)_6\} + E\{H_2O\} - E\{M(H_2O)_7\}$. ^d Difference in hydration enthalpy calculated using the Born equation (ref 22) for $R_7 + R(\text{H}_2\text{O})$ and $R_6 + R(\text{H}_2\text{O})$, with $R(\text{H}_2\text{O}) = 1.40 \text{ \AA}$, $\epsilon(\text{H}_2\text{O}) = 78$, and $T\epsilon^{-1}(\partial\epsilon/\partial T) = -1.357$ for water at 298 K (ref 23). ^e Calculated associative activation enthalpy (kJ mol^{-1}) $\Delta H_{\text{ass}}^e = -\Delta E_7 + \Delta H_{\text{vap}} + \Delta H_{7-6}^{\text{soliv}}$ (see eq 2). ^f Experimental activation enthalpy (ref 4). ^g Calculated including CAS corrections (see Methods). ^h D_{3d} symmetry (see ref 9).

with an essentially associative mechanism for Ti^{3+} , which gradually becomes more intermediate in character for V^{3+} , Fe^{3+} , and Cr^{3+} , and attains a dissociative character for the grossly deviating Ga^{3+} ion, as discussed below. It is generally agreed that the fairly large hexahydrated Ti^{3+} ion with its strongly negative activation volume (Table 3) follows an essentially associative interchange mechanism in its water exchange.^{3,4} This is also supported by the high relative stability of its heptahydrate (see Figure 3). The bond energy difference from the dashed line in Figure 4d with a slope $RT \ln 10$ of 5.70 kJ mol^{-1} (corresponding to $T = 298 \text{ K}$) passing through the Ti^{3+} value can then be used as an approximate measure of the decrease in the activation energy by the increasing interchange contribution as compared to an associative mechanism for the V^{3+} , Fe^{3+} , and Cr^{3+} ions. Their sizes are closely similar for the heptahydrates (R_7 in Table 2), but the Cr^{3+} ion has a smaller hexahydrate (Figure 2), which gives it a higher solvation energy and also a higher activation enthalpy (the increase in $\Delta H_{7-6}^{\text{soliv}}$ is estimated to be ~ 11 – 16 kJ mol^{-1} , Table 4). In solution the hexahydrated state of Cr^{3+} would probably be further stabilized by the strong hydrogen bonding,²⁰ thus giving an additional reduction of the associative character of the exchange reaction.

For the divalent ions, no correlation can be found between an associative gas-phase process and the experimental water-exchange rates, in sharp contrast to the satisfactory correlation found for the dissociative mechanism, cf. Figure 4a,b. This further supports our previous conclusion that the divalent ions (V^{2+} – Zn^{2+}) all react through a dissociative mechanism regardless of the sign and magnitude of the experimental ΔV^* value.⁷

The formation of heptahydrates from the hexahydrated complexes is accompanied by bond elongations of similar magnitude for both the di- and trivalent ions: $\Delta R \approx 0.1 \text{ \AA}$, although somewhat more uniform for the trivalent ions (Table 4). These expansions are significantly larger than the contractions

(20) Bergström, P.-Å.; Lindgren, J.; Read, M.; Sandström, M. *J. Phys. Chem.* 1991, 95, 7650.

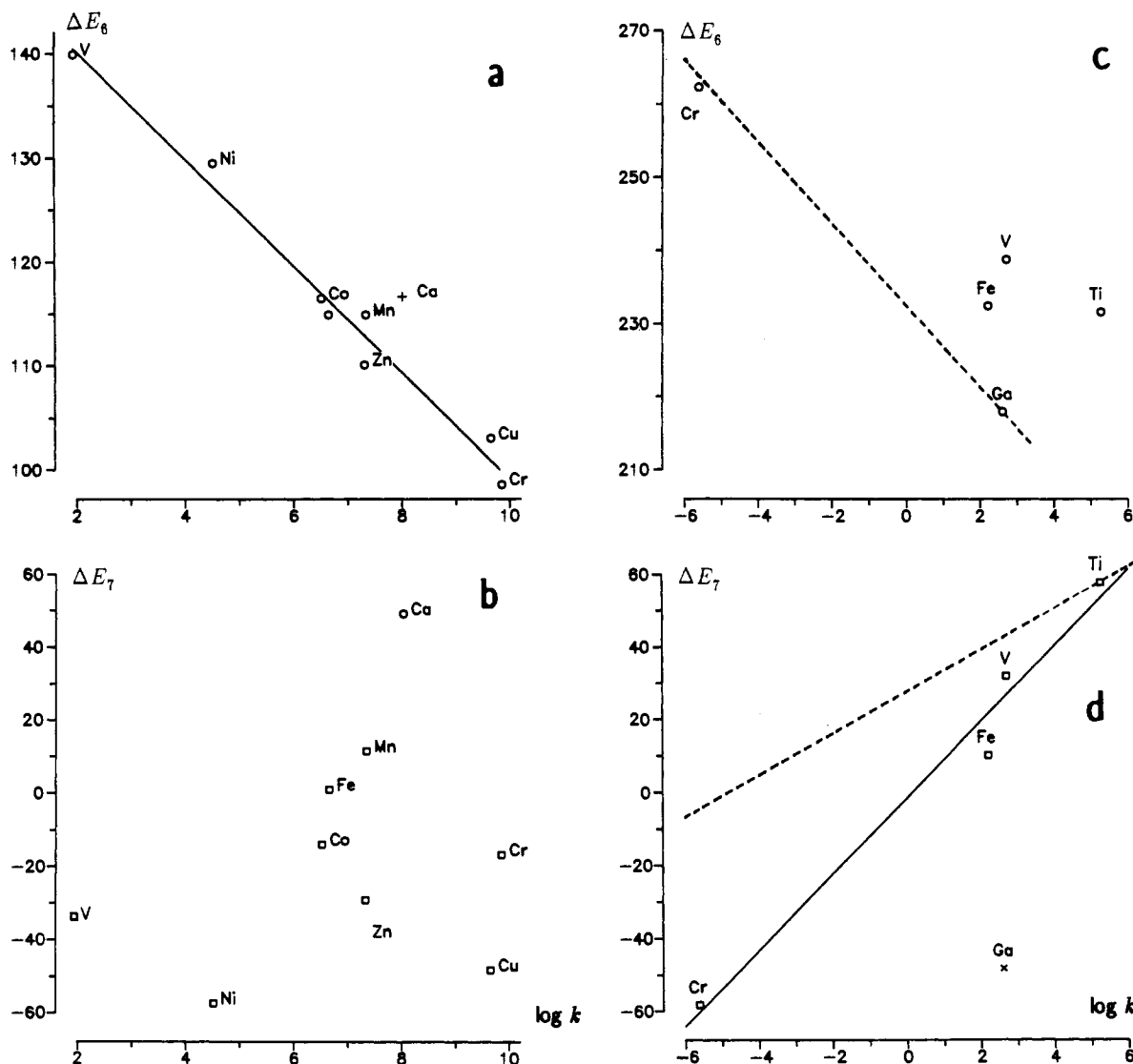


Figure 4. Tests of dissociative or associative character of the reactions by Arrhenius plots (see text) of bond dissociation energies ΔE_n (in kJ mol^{-1}) versus the logarithm of the experimental water-exchange rate constants (in s^{-1}), $\log k$, of the hexahydrated 3d ions: (a) M^{2+} , dissociation to pentahydrates (Ca^{2+} excluded, see text); (b) M^{2+} , association to heptahydrates; (c) M^{3+} , dissociation to pentahydrates; (d) M^{3+} , association to heptahydrates (Ga^{3+} excluded from correlation line, see text). The dashed lines correspond to idealized reaction mechanisms at 298 K.

at the formation of pentahydrates: $\Delta R \approx 0.04 \text{ \AA}$ (Table 3). Larger energy contributions are therefore obtained using the Born model to describe the energy of solvation of the activated complex in an associative mechanism (cf. Tables 3 and 4 and the discussion below). The relatively large expansions of the volume at the formation of the heptahydrated complex ($\Delta V_{7-6}^* \approx 10 \text{ cm}^3 \text{ mol}^{-1}$, Table 4) would in solution be further enhanced by the weakening of the hydrogen bond formation. Infrared spectroscopic measurements show that the hydrogen bond strength of the probably about seven water molecules in the first shell around Ca^{2+} in aqueous solution is weaker than that in bulk water (the strength is similar to that of a group of weakly hydrated mostly uni- and large divalent ions), while most hexahydrated divalent ions form a group with somewhat stronger hydrogen bonds (see the discussion in ref 7), and also that a stepwise increase occurs to a group with appreciably stronger hydrogen bonds for the small (e.g., Cr^{3+} and Rh^{3+}) hexahydrated trivalent ions.²⁰ This groupwise similarity of the hydrogen bond strength could be a reason for the success of the applied gas-phase model, which assumes constant differences between the energy contributions from the solvent in the initial and transition states.

For the dissociative mechanism, a similar reasoning can be made, where the expected increase in hydrogen bond strength for

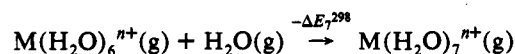
the pentahydrated species would further increase the volume contraction in the transition state.⁷ These contributions to the intrinsic volume change would then act in different directions in dissociative and associative water-exchange processes and again illuminate the difficulty in using the experimental ΔV_{exp}^* values as direct indicators of the proposed mechanism by assuming that no bond length variations occur at the transition state.³ Generally, it seems that the interchange mechanism for a water-exchange reaction with a small or slightly negative ΔV_{exp}^* value has a more dissociative character than proposed previously.³

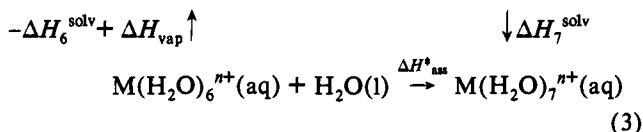
III. Activation Enthalpies. Experimental ΔH^* enthalpy data exist for five of the M^{3+} and also for five of the M^{2+} ions in this study and can be compared to the calculated dissociation energies, assuming pure dissociative or associative interchange, with the use of a Born-Haber cycle at 298 K. The dissociative process has been treated in ref 7b and gives in the present notation:

$$\Delta H_{\text{diss}}^* = \Delta E_6^{298} + \Delta H_5^{\text{solv}} - \Delta H_6^{\text{solv}} - \Delta H_{\text{vap}} \quad (1)$$

For the associative process, the Born-Haber cycle below gives

$$\Delta H_{\text{ass}}^* = -\Delta E_7^{298} + \Delta H_7^{\text{solv}} - \Delta H_6^{\text{solv}} + \Delta H_{\text{vap}} \quad (2)$$





where the experimentally derived ΔH^* values ideally should fall between the calculated estimates of the ΔH^*_{diss} and ΔH^*_{ass} values (Tables 3 and 4). The heat of vaporization of water is $\Delta H_{\text{vap}} = 44.02 \text{ kJ mol}^{-1}$ (298 K).²¹ The solvation enthalpy ΔH_6^{solv} of a hexahydrated trivalent ion, $\text{M}(\text{H}_2\text{O})_6^{3+}(\text{g}) \rightarrow \text{M}(\text{H}_2\text{O})_6^{3+}(\text{aq})$, can be estimated from the difference between the total binding energy of the hexahydrated complex and the experimental single-ion hydration enthalpies, and values in the range ca. 2096–2256 kJ mol^{-1} were obtained for the ions in this study.⁹ The ΔH_6^{solv} values for the divalent ions range from ca. 926 to 1020 kJ mol^{-1} .^{7a,9} The Born equation, $\Delta H_{\text{Born}} = -q^2\{1 - \epsilon^{-1} - T\epsilon^{-2}(\partial\epsilon/\partial T)\}/8\pi\epsilon_0 r$, giving the enthalpy of solvation for an ion (radius r) in a structureless dielectric continuum (dielectricity constant ϵ),²² has been used to estimate the difference in the contributions in solvation energy between the hexahydrate and the activated complexes. Despite its approximate nature, the effects of its deficiencies (solvent polarization and entropy contributions, non-zero multipole moments, etc.) will be largely eliminated because of the relatively small differences in the applied mean radii, $r_1 = R_5 + R(\text{H}_2\text{O})$, $R_6 + R(\text{H}_2\text{O})$, and $R_7 + R(\text{H}_2\text{O})$ with $R(\text{H}_2\text{O}) = 1.40 \text{ \AA}$.^{22–24}

Relatively minor corrections are needed to adjust the calculated gas-phase dissociation energies ΔE from 0 to 298 K,⁹ i.e. differences in zero-point energies, heat capacities, and volume changes of the reactants, and the remaining discrepancy between the experimental and theoretical ΔH^* values should mainly be due to deficiencies in the computational models. Changes in electron correlation, spin-orbit coupling, and basis set errors including corrections for relativistic effects of the metal ions would contribute to some extent but probably be less important than the electronic and geometrical relaxation of the solute in solution,^{24–26} where, for example, the metal–oxygen bond length and water ligand geometry of the hydrated complexes will be influenced by the polarization and hydrogen bonding.⁹

Nevertheless, in a series of similar species, a comparison of the trends of the calculated and experimental activation enthalpies is of interest. Plots of the differences $\Delta H^*_{\text{diss}} - \Delta H^*$ and $\Delta H^*_{\text{ass}} - \Delta H^*$ are given in Figure 5. The divalent 3d ions show rather small remaining values with a more constant discrepancy $\Delta H^*_{\text{diss}} - \Delta H^*$ (16–34 kJ mol^{-1}) than for $\Delta H^*_{\text{ass}} - \Delta H^*$. For the trivalent ions, the enthalpies for the dissociative mechanism give much larger deviations from the experimental activation enthalpies than from the associative (except for Ga^{3+}). The smallest deviation is obtained for the associative enthalpies of Ti^{3+} and V^{3+} : it increases for Fe^{3+} and Cr^{3+} and deviates grossly for Ga^{3+} . This gives an overall picture consistent with the scheme proposed above (see Associative Mechanism) based on the Arrhenius plots, with interchange mechanisms of dissociative character for Ga^{3+} and with gradually increasing associative character for the remaining ions in the order Cr^{3+} , Fe^{3+} , V^{3+} , and Ti^{3+} .

The high degree of correlation between ΔE_6 and $\log k$ gives strong support to a dissociative mechanism for the divalent ions.^{7b} The rather constant difference $\Delta H^*_{\text{diss}} - \Delta H^*$ thus indicates that there are further contributions needed to obtain theoretical ΔH^* values fully comparable with the experimental ΔH^* parameters. For a dissociative reaction in solution, the increased electronic polarization and the increase in hydrogen bond strength to the second hydration shell should become significantly stronger in

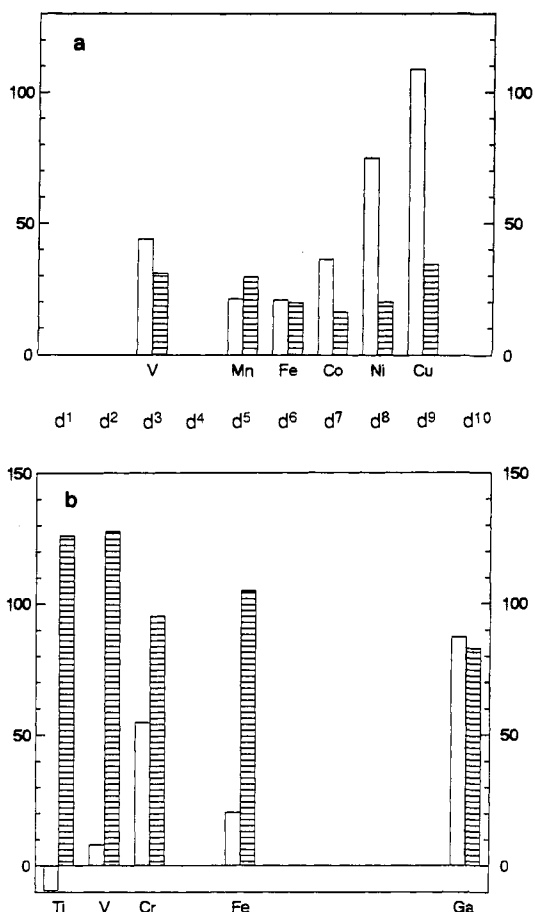


Figure 5. Activation enthalpy differences $\Delta H^*_{\text{ass}} - \Delta H^*$ (open staples) and $\Delta H^*_{\text{diss}} - \Delta H^*$ (striped staples) in kJ mol^{-1} for (a) divalent 3d ions (upper part) and (b) trivalent 3d ions (lower part).

the transition state due to the shortening of the M–O bonds.^{7b,9,20} A model accounting for these effect would give lower calculated values and reduce the difference $\Delta H^*_{\text{diss}} - \Delta H^*$.

Thus, in evaluating the intermediate dissociative or associative character of the interchange reactions, based on the magnitude of the differences between the ΔH^* values in Figure 5, this contribution should favor the dissociative mechanism. As a consequence, the Ga^{3+} ion would be more dissociative (as expected) than the almost equal values of ΔH^*_{diss} and ΔH^*_{ass} now indicate and also the Cr^{3+} ion would have a more intermediate (but still associative) interchange character than Fe^{3+} , as discussed above.

The calculated energy barriers of Ga^{3+} for bond making/breaking differ significantly from those of the other M^{3+} ions, which probably is related to the larger degree of covalency in the Ga– H_2O bonds.⁹ The different behavior of Ga^{3+} is also illustrated by the metal atom charges obtained for the penta-, hexa-, and heptahydrated complexes of Sc^{3+} , Ti^{3+} , V^{3+} , Cr^{3+} , Mn^{3+} , Fe^{3+} , and Ga^{3+} from Mulliken population analyses of calculations with the large water basis sets. The first five ions have their highest charge in the hexahydrate, and for Fe^{3+} , the charge decreases with increasing coordination number whereas for Ga^{3+} the charge increases from +2.00 (penta-) to +2.02 (hexa-) and +2.25 (heptahydrate).

Concluding Remarks. The variation of the reaction rates of water exchange for the divalent first row transition metal ions can be satisfactorily described theoretically by a model assuming a pentahydrated transition state corresponding to a dissociative interchange mechanism. However, the results for the trivalent 3d ions are consistent with an associative interchange with gradually increasing intermediate character for Ti^{3+} , V^{3+} , Fe^{3+} , and Cr^{3+} and a dissociative interchange mechanism for Ga^{3+} . The volume and energy changes in the transition state follow

(21) *American Institute of Physics Handbook*; Gray, D. E., Ed.; McGraw-Hill: New York, 1972.

(22) Bockris, J. O'M.; Reddy, A. K. N. *Modern Electrochemistry*; Plenum: New York, 1970; Vol. 1, Chapter 2.

(23) Rashin, A. A.; Honig, B. J. *Phys. Chem.* **1985**, *89*, 5588.

(24) Bertrán, J.; Ruiz-Lopez, M. F.; Rinaldi, D.; Rivail, J. L. *Theor. Chim. Acta* **1992**, *84*, 181.

more similar trends for the associative interchange processes of the trivalent 3d ions than for the dissociative exchange of the divalent 3d ions. The compaction of the hexahydrated complex and its entering water molecule necessary to achieve the transition state (which is inherent in the measured activation volumes ΔV^*_{exp}) does not follow the energy profile of bond breaking for the early divalent 3d ions. The differences in bond elongation, hydrogen bonding, and also the degree of penetration into the first shell of the incoming water before bond breaking occurs seem to be more uniform for the trivalent ions. Positive ΔV^*_{exp} values seem to be more reliable as indicators of dissociative interchange mechanisms than negative ΔV^*_{exp} values of small magnitude for predicting associative behavior.

The models used in the present work assume similar changes in the energy contributions from the surrounding solvent along the water-exchange reaction path within a series of ions. This approach is justified by the satisfactory correlation for the divalent 3d ions. Of general interest is that this seems to corroborate the underlying assumption of similarity between the collisional model for activation in the gas phase and in liquid solutions. The next step in verifying the energetics of the proposed types of reaction

in solution would be to include the solvent influence in the computational procedure on the electronic and geometrical relaxation of the solute. A tractable procedure for this purpose seems to be the supermolecule and cavity model employed by, for example, Rivail and co-workers describing the solvent as a polarizable and dielectric continuum surrounding the cavity where the solute is located.²⁴⁻²⁶ However, cavity sizes and shapes are important for a good account of the induced polarizability and of multipole interactions (which may influence the SQP-TBP relative stability). In particular, the description of the hydrogen bonding, which tends to become underestimated with this model,²⁶ is critical and might require a large supermolecule inside the cavity for a satisfactory description.

Acknowledgment. The financial support and the CPU time on a CRAY-XMP/416 obtained through the Swedish Natural Science Research Council are gratefully acknowledged.

(25) Sánchez Marcos, E.; Pappalardo, R. R.; Rinaldi, D. *J. Phys. Chem.* **1991**, *95*, 8928.

(26) Tuñón, I.; Silla, E.; Bertrán, J. *J. Phys. Chem.* **1993**, *97*, 5547 and references therein.